Physicochem. Probl. Miner. Process., 57(5), 2021, 57-70

http://www.journalssystem.com/ppmp

Physicochemical Problems of Mineral Processing

ISSN 1643-1049

Received April 12, 2021; reviewed; accepted July 19, 2021

New insights into the promotion mechanism of $(NH_4)_2SO_4$ in sulfidization flotation: a combined experimental and computational study

Daixiong Chen [1,2,4], Mengfei Liu [2], Bo Hu [1,3], Yanhong Dong [1], Wei Xue [1], Peng He [2], Fang Chen [2], Jianyu Zhu [2,4], Chenyang Zhang [2]

[1] Hunan Provincial Key Laboratory of Complex Copper Lead Zinc Associated Metal Resources Comprehensive Utilization, Hunan Research Institute for Nonferrous Metals, Changsha 410100, China

[2] School of Minerals Processing and Bioengineering, Key Laboratory of Biometallurgy of Ministry of Education, Central South University, Changsha 410083, China

[3] College of Resource and Environmental Engineering, Wuhan University of Science and Technology,

[4] State Key Laboratory of Comprehensive Utilization of Low-Grade Refractory Gold Ores, Zijin Mining Group Co., Ltd, Shanghang 364200, China

Corresponding authors: zhujy@csu.edu.cn (J. Zhu), zhangchenyang@csu.edu.cn (C. Zhang)

Abstract: Ammonium sulfate ($(NH_4)_2SO_4$) exhibits promoting effects in malachite sulfidization flotation. However, the promotion mechanism remains poorly understood. In this study, micro-flotation tests, zeta-potential measurements, scanning electron microscopy coupled with energy-dispersive spectroscopy (SEM-EDS), atomic force microscopy (AFM), X-ray photoelectron spectroscopy (XPS) and materials studio simulation (DFT) were used to investigated the promotion mechanism of $(NH_4)_2SO_4$. Micro-flotation test demonstrates that the recovery of malachite from 73% increased to 83%, when the $(NH_4)_2SO_4$ was added. Contact angle and zeta potential test results indicate that addition of $Na_2S·9H_2O$ changes the surface properties of malachite and provide the conditions for adsorption of butyl xanthate (BX). After promoting the sulfidization by $(NH_4)_2SO_4$, BX is more effective in improving the hydrophobicity. SEM-EDS and AFM results show that $(NH_4)_2SO_4$ can improve performance and stability of sulfidization. X-ray photoelectron spectroscopy indicates that after sulfidization, polysulfides and cuprous were appeared in malachite surface, infers that a redox reaction occurs between sulfur and copper on the surface of malachite. After addition of $(NH_4)_2SO_4$, the percentage of polysulfides and cuprous were increased, it implies $(NH_4)_2SO_4$ can accelerate the redox reaction. Computational results show that after adding $(NH_4)_2SO_4$, the adsorption energy of HS^- on the malachite surface is reduced, implies that $(NH_4)_2SO_4$ can improve the stability of HS^-adsorption on the surface of malachite.

Keywords: malachite, promotion, sulfidization, flotation, mechanism

1. Introduction

Copper possesses excellent electrical and thermal conductivity, as well as ductility, and is a significant industrial metal (Tran et al., 2020). In nature, copper occurs primarily in the form of sulfide ores (Cao et al., 2009). At present, sulfide ore is the main source of copper. However, with the depletion of sulfide ore resources, many scholars are focusing on the utilization of copper oxide ores. Copper oxide minerals include malachite ($Cu_2(OH)_2CO_3$), azurite ($2CuCO_3·Cu(OH)_2$), chrysocolla ($CuSiO_3·2H_2O$) (Tanda et al., 2017), brochantite ($CuSO_4·3Cu(OH)_2$), and bluestone ($CuSO_4·5H_2O$) (Corin et al., 2017; Feng et al., 2015; Frost et al., 2012). Malachite is a typical mineral of copper oxide with characteristics such as strong hydrophilicity, sliming, and complex mineral composition. The development and utilization of copper

DOI: 10.37190/ppmp/140340

oxide mainly focus on the utilization of malachite. Therefore, the efficient recovery of malachite is a popular research topic in the field of mineral processing.

Froth flotation is an effective separation technique for recovering copper oxide minerals (Nagaraj and Farinato, 2016). In this process, the targeted mineral particles in an aqueous pulp become attached to air bubbles to form particle/bubble aggregates, which are transported out of the pulp (Liu et al., 2020). In present, direct flotation and sulfidization flotation are used for extracting copper oxide (Wu et al., 2017a). For direct flotation, chelating agents such as flotation collectors are employed to float copper oxide minerals. The interaction mechanism between the chelating agents and the mineral surfaces has been investigated using solution measurements, surface analysis techniques, and density functional theory calculations (Fuerstenau et al., 2000; Li et al., 2017; Yang et al., 2017). Several researchers have focused on synthesizing effective chelating agents to achieve the efficient flotation of copper oxide minerals. Alkyl hydroxamates (Lee et al., 1998), aldoximes (Xu, 1989), and n-octanohydroxamate (Hope et al., 2012) has proven to be suitable collectors. These reagents exhibit a superior affinity for copper oxide minerals but poor selectivity for gangue minerals. Sulfidization xanthate flotation is the most widely used method for recycling malachite (Castro et al., 1974; Shengo et al., 2014). When malachite interacts with sulfidizing agents, the properties of malachite are altered, hence, xanthate can be adsorbed on the sulfided area. The mechanism of sulfidization processing involves the ionization of sodium sulfide in water to produce HS^- and S^{2-} ions, which undergo chemisorption with copper ions on the surface of copper oxide minerals. *Hu* et al (Hu et al., 1996). studied the kinetic potential of malachite and found that HS^- ions are the main component of sodium sulfide on the surfaces of malachite. *Liu* et al (Liu et al.,2020). concluded that sulfidization of malachite is a phase-transition process driven by the solubility difference between $Cu_2(OH)_2CO_3$ and Cu_2-xS, Cu_2-xS phases formation on malachite involves heterogeneous nucleation and growth. However, various surface tensions and imperfections on the surfaces of the malachite increase the uncertainty for sulfidization flotation, because xanthate can be adsorbed in the sulfurized zone, and it is not easily adsorbed in the semi-sulfurized and non-sulfurized zones (Ejtemaei et al., 2014; Naklicki et al., 2002), therefore, sulfidization is a critical stage for the sulfidization xanthate flotation of malachite. Moreover, an inadequate amount of sulfidation reagents cause a restricted improvement to malachite flotation recoveries, an excessive HS^-/S^{2-} can also act as a strong inhibitor (Zhang, 2008).

Sulfidization Flotation is an efficient method for separating malachite from gangue minerals. However, sulfidization process is relatively unstable, sulfidization time and dosage of sulfurizing reagent will have a greatly influence on the sulfidization flotation effect. (Castro et al., 1974). The stabilization of sulfidization flotation could be improved using the accelerant. Ammonium sulfate is one of the most common accelerants used in sulfidization flotation. Many scholars have explored the promotion mechanism of ammonium sulfate in sulfidation flotation. Previously, *Zhang* et al (Zhang et al., 1989). suggested that ammonium sulfate can accelerating the sulfidization rate and improving the stability of sulfidization product layer. Recently, *Shen* et al (Shen et al., 2019). demonstrated that $(NH_4)_2SO_4$ can eliminating the depression of excess S^{2-}. *Liu* et al (Liu et al., 2018). according to SEM-EDS results indicated that $(NH_4)_2SO_4$ promoted more S element absorbed and distributed equality on the malachite surface, but there is no indication of the intuitive morphology of surface sulfides. *Liu* et al (Liu et al., 2020). confirmed the sulfidization product grown on malachite were the copper-deficient Cu_2-xS phases, ammonium was mediate the nucleation and growth of the sulfidization product during malachite sulfidization. All those studies well reveal the role of ammonium ions in the formation of sulfides.

Despite a substantial effort to ascertain the action of ammonium sulfate in the sulfidation flotation, there is currently no exact mechanism. In this study, contact angle measurements, scanning electron microscopy (SEM), X-ray photoelectron spectroscopy (XPS), atomic force microscopy (AFM) and computational chemistry were carried out to reveal the promotion mechanisms of ammonium sulfate on sulfidization flotation and to elucidate the internal interaction between mineral and agents.

2. Experiment

2.1 Minerals and reagents

The malachite samples used in this study were obtained from Yunnan Province, China. The mineral

samples were ground in a porcelain ball mill and screened to obtain a fractional size of -0.074 mm, which was used in the micro-flotation experiments. The results of X-ray fluorescence (XRF) and X-ray diffraction (XRD) analyses are presented in Table 1 and Fig 1.

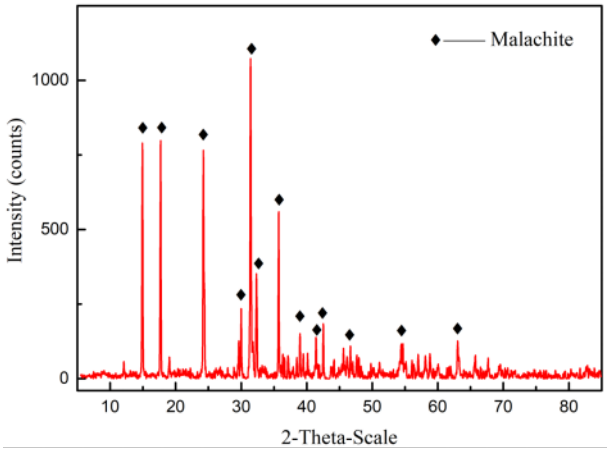

Fig. 1. XRD pattern of pure malachite mineral

Table 1. XRF analysis of pure minerals used in these experiments

Element	Cu	Fe	Zn	Hf	Others
Concentration (%)	56.592	0.078	0.146	3.001	40.183

Fig. 1 and Table 1 indicate that the sample features high purity. Analytical-grade $(NH_4)_2SO_4$ was used as an accelerant, and analytical-grade $Na_2S \cdot 9H_2O$ was used as a sulfurizing reagent. Industrial-grade butyl xanthate (BX) and terpineol were used as the collector and frother, respectively. Pure hydrochloric acid (HCl) and sodium hydroxide (NaOH) were used as the pH regulators, and deionized water was used in all the tests.

2.2. Flotation tests

The flotation experiments were performed in XFG-type flotation cells, with 10 g of malachite samples used in each experiment. The samples were placed in a 150 cm^3 flotation cell and the pH was adjusted (if required) for flotation. First, the $(NH_4)_2SO_4$ was added and the mixture was conditioned for 1 min. Immediately, $Na_2S \cdot 9H_2O$ was added and the mixture was stirred for 2 min. Thereafter, industrial-grade BX was added and stirred for 1 min followed by the addition of an industrial-grade frother, terpineol, and again stirred for 1 min. The flotation scratch runs were conducted for 3 min. The foam was collected, dried, and analyzed. All flotation experiments were repeated under the same conditions. The steps of the flotation experiments are depicted in Fig. 2.

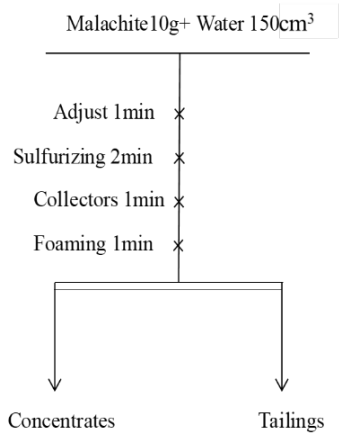

Fig. 2. Process flow of flotation

2.3. Contact angle measurements

Pure malachite minerals were cut into small pieces and then polished to obtain shiny surfaces. Thereafter, the minerals were immersed in deionized water for 5 min under ultrasonic vibration then treated with 4×10^{-4} mol/L $(NH_4)_2SO_4$ and 3×10^{-3} mol/L $Na_2S \cdot 9H_2O$ solutions. Subsequently, 4×10^{-4} mol/L butyl xanthate as collector were added. Finally, the pieces were removed from the solution and dried in a vacuum. The contact angle of the liquid on the surface of the mineral crystal was measured using the pendant drop method on a DSA30 contact angle measuring instrument (KRUSS, German) and the circle fit was used for the contact angle calculations. The measuring instrument was equipped with a manual dropping system, high-performance CCD video camera, and software that calculates the corresponding contact angle based on the shape of the droplet on the surface of the mineral. The accuracy of the measurement was ±2°.

2.4. Zeta potential measurements

The mineral sample was ground to a particle size of 2 μm with an agate mortar. Thereafter, 0.2 g of the sample was added to a 100 cm^3 beaker filled with 50 cm^3 of deionized water containing 5×10^{-3} mol/L KNO_3 background solution and stirred with a magnetic stirrer for 2 min. The pH was adjusted using HCl or NaOH. At the pH of the slurry, 4×10^{-4} mol/L $(NH_4)_2SO_4$, 3×10^{-3} mol/L $Na_2S \cdot 9H_2O$ and 1×10^{-4} mol/L butyl xanthate were added. The suspension was allowed to settle for 10 min. The supernatant was collected for testing. It was injected into the electric pool of the Zetasizer Nano Zs90 potential analyzer (Malvern Panalytical, Malvern, UK) to measure the potential. Each sample was measured three times and the average value was calculated.

2.5. Scanning electron microscopy

The preparation and testing methods used for the ore sample and medicament ore sample are as follows: 2 g of pure mineral (of particle size -0.074 mm) and 30 cm^3 of deionized water were added to a beaker and stirred for 1 min. When required, 4×10^{-4} mol/L $(NH_4)_2SO_4$ was added into the suspension and stirred for 1 min. Thereafter, the prepared 3×10^{-3} mol/L $Na_2S \cdot 9H_2O$ solution was added to the mixture stirred for 1 min. Next, the ore samples were removed from the beaker and dried in a vacuum drying box at 298.15K. Scanning electron microscopy (SEM; TESCAN MIRA3 LMU) in conjunction with energy-dispersive spectroscopy (EDS; Oxford X-Max20) was conducted to observe the surface topography of malachite in the absence and presence of $Na_2S \cdot 9H_2O$ or $(NH_4)_2SO_4$.

2.6. Atomic force microscopy

The sample preparation as follows: a piece malachite was cut and polished to produce 2×2×1mm lamelliform samples. Then, the prepared malachite samples were put into an Erlenmeyer flask and add 150 deionized waters. Thereafter, the accelerant and the sulfidizing agent was added to Erlenmeyer flask. Immediately, transfer the Erlenmeyer flask to the shaker and shake 3nin at 25°C and 100 rpm. After that, take the sample out, and dry in a vacuum drying chamber. The AFM test was conducted in a multi-mode SPM AFM (Veeco Instruments, Inc., USA) at 298.15K. The outline of the original image was processed using Nanoscope 7.3 software (Bruker, Santa Barbara, CA, USA).

2.7. X-ray photoelectron spectroscopy

The samples were prepared using the same method as for the SEM-EDS analysis. Thereafter, the SIGMA PROBE multifunctional electronic spectrometer with Al Ka (1486.6 eV) as the emission source was used. Scanning was performed using a low-energy electron neutralization method with a scanning area of 400 μm and vacuum degree less than 5×10^{-10} mbar. The test conditions (narrow scan) were as follows: pass energy of 50 eV, step size of 0.1 eV, and dwell time of 50 ms.

2.8. Computational method

The crystal structure model of malachite was obtained from the American Mineralogist Crystal Structure Database. The interaction between the HS^- ions and malachite (-2 0 1) surface in the absence

and presence of the NH_4^+ was simulated using the CASTEP program, a quantum chemistry module of Materials Studio (Clark et al., 2005). In this study, the exchange correlation function used the PW91 gradient correction function under GGA to provide a description and the ultrasoft pseudopotential of the PW base cluster to describe the interaction between the ion core and the valence electron (Wu et al., 2017b). The total system energy and charge density were subjected to integral calculation in the Brillouin zone using the Monkhorst–Pack scheme. The cut-off energy was set to 381 eV. The size of the selected k-grid point was 1 × 1 × 1. In a self-consistent field operation using the Pulay density mixture method, the convergence accuracy was set to 2.0×10^{-5} eV/atom. The BFGS algorithm was utilized to optimize the model structure. The convergence criteria for the interaction forces between atoms, internal stress of the crystal, and maximum atomic displacement were set to 0.005 eV nm^{-1}, 0.1 GPa, and 0.002 Å, respectively.

3. Results and discussion

3.1. Flotation tests

3.1.1. The flotation behavior of malachite as a function of Na_2S concentration

Sulfidizing agent can change the properties of malachite surface, makes it easier for xanthate to adsorb on the surface. The effects of $Na_2S \cdot 9H_2O$ dosage on the sulfidization flotation of malachite are depicted in Fig. 3. The experiments are carried out at natural pH and the amount of BX was fixed at 1×10^{-3} mol/L.

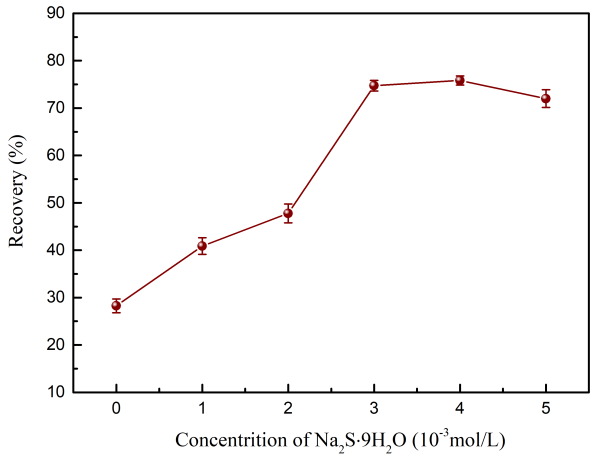

Fig. 3. Malachite flotation experiment as function of Na2S concentration

It can be concluded from Fig. 3 that an increased amount of $Na_2S \cdot 9H_2O$ (within 3×10^{-3} mol/L) leads to a higher recovery rate of malachite, to a peak value of 75%. However, this was followed by a downward trend, which implies that excessive sulfidizing agent can inhibit the flotation of malachite.

3.1.2. The flotation behavior of malachite as a function of butyl xanthate concentration

In earlier experiments, the relationship between the optimum amount of collector BX and recovery rate of malachite was investigated. In this experiment, the concentration of $Na_2S \cdot 9H_2O$ is 3×10^{-3} mol/L and the pH is 9.5.

Using BX as a collector, the flotation recovery of malachite as a function of BX concentration in the absence and presence of $Na_2S \cdot 9H_2O$ is depicted in Fig. 4. For malachite flotation without $Na_2S \cdot 9H_2O$, the recovery increased with increasing the amount of BX, but the overall recovery was lower. After adding $Na_2S \cdot 9H_2O$, the recovery rate gradually increased. When the amount of the collector was 8×10^{-4} mol/L, the recovery rate reached the maximum of 75%. The recovery of malachite did not change significantly when the amount of the collector was increased further.

3.1.3 Promotion of malachite sulfidation flotation by ammonium sulfate

We also studied the effect of the amount of $(NH_4)_2SO_4$ on the recovery of malachite flotation. In this experiment, the pH was 9.5±0.2, the dosages of collector and $Na_2S \cdot 9H_2O$ were 1×10^{-4} and 3×10^{-3} mol/L, respectively. Fig. 5 clearly indicates that the recovery of malachite gradually increased from 73% to 82% in the presence of $(NH_4)_2SO_4$. When the amount of $(NH_4)_2SO_4$ was 4×10^{-4} mol/L, the recovery of malachite reached the maximum of 82% and then started to decline.

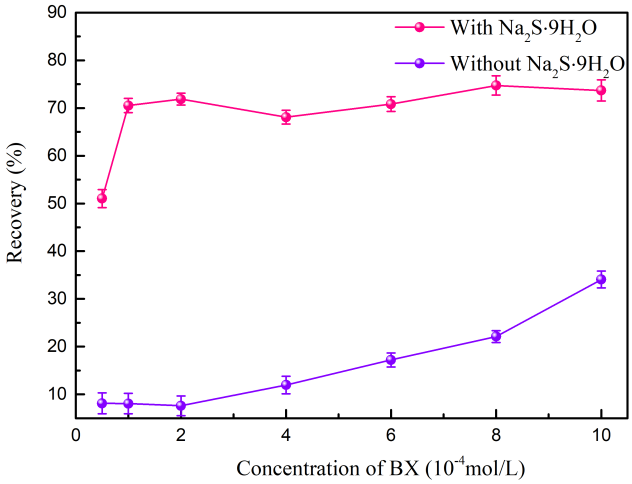

Fig. 4. Flotation experiments on malachite as function of BX concentration

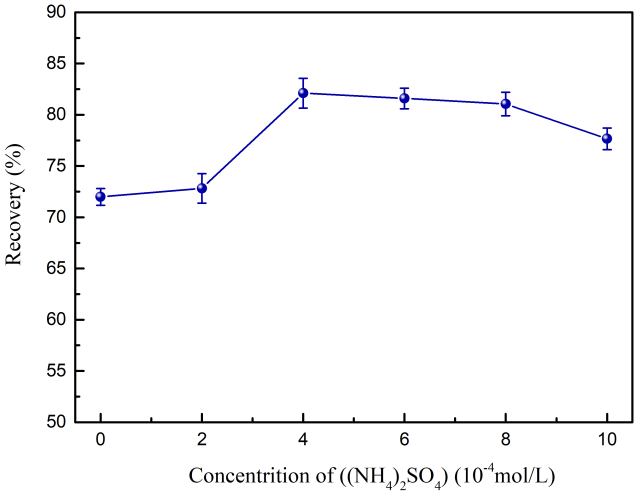

Fig. 5. Effect of $(NH_4)_2SO_4$ concentration on malachite flotation

3.1.4. The sulfidization flotation behaviour of malachite in presence $(NH_4)_2SO_4$ as a function of pH

The relationship between the recovery of sulfidization flotation and the pH of the pulp in the presence or absence of $(NH_4)_2SO_4$ was experimentally studied. The amounts of $(NH_4)_2SO_4$, $Na_2S \cdot 9H_2O$, and the collector BX were fixed at 4×10^{-4}, 3×10^{-3}, and 1×10^{-4} mol/L, respectively. The pulp pH was adjusted with hydrochloric acid and sodium hydroxide. It can be seen from Fig. 6 that without $(NH_4)_2SO_4$, the recovery of malachite increased at pH levels of 6–9; at pH levels above 9, the recovery rate gradually decreased. At a pH of 9, the recovery rate was the highest at 74%. The recovery rate of malachite was higher with the addition of $(NH_4)_2SO_4$ rather than without; the highest recovery was 85% at a pH of 11. Over that the recovery continued to decrease as the pH increase.

3.2. Study on promotion mechanism of malachite sulfidization flotation

3.2.1. Contact angle measurements

Through the contact angle test, the effect of the amount of BX on the hydrophobicity of the surface of malachite before and after sulfidation was explored.

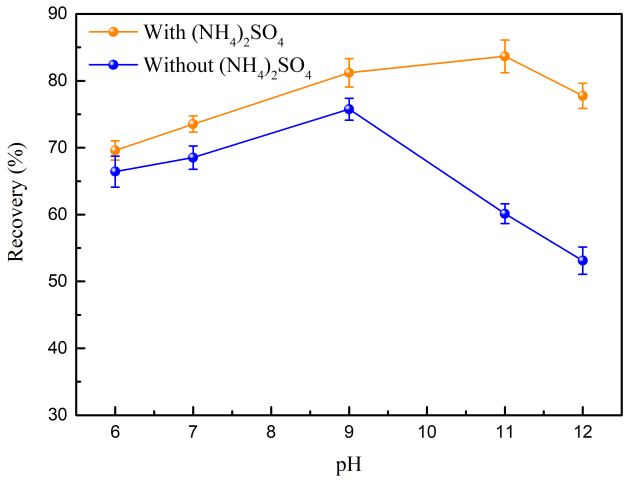

Fig. 6. Relationship between pH and recovery rate of malachite sulfidization flotation in in the presence or absence of $(NH_4)_2SO_4$

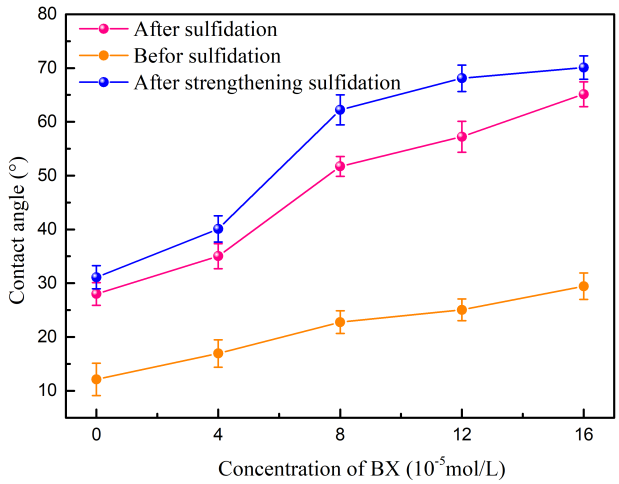

Fig. 7. Contact angles of malachite as function of BX dosages in the absence and presence of $(NH_4)_2SO_4$ and Na_2S

It can be seen in Fig. 7 that before sulfidization, the surface of malachite was strongly hydrophilic, with a surface contact angle of approximately 13°. After the addition of BX, the contact angle increased. It means that the addition of sulfidizing agent changes the surface properties of malachite and improves its hydrophobicity. Before sulfidization, with the increased of xanthate concentration, the contact angle increased slowly. After sulfidization, the contact angle of the surface of malachite without the addition of BX was 28°. With an increase in the concentration of BX, the contact angle increased significantly. When the amount of BX was increased to 16×10^{-4} mol/L, the contact angle of the surface of malachite was 66°. When $(NH_4)_2SO_4$ was added to strengthen the sulfidization, the contact angle of the surface of malachite was larger when it compared with that for direct sulfidization. Doubtlessly, this was due to that more BX adsorbs on the surface of malachite, thereby increasing its hydrophobicity. The result indicates that after strengthening the sulfidization treatment of malachite, BX is more effective in improving the hydrophobicity of its surface, this is conducive to flotation.

3.2.2. Zeta potential measurements

The zeta potential test was conducted to explore the effect of reagents on the electrical properties of the surface of malachite under various conditions.

The zeta potentials of malachite were measured in the absence and presence of $(NH_4)_2SO_4$, $Na_2S \cdot 9H_2O$ and BX, and the results are presented in Fig. 8. For original malachite, when the pH was in the range of 3–7, the zeta potential was positive. At pH levels above 7, the zeta potential was negative, and the isoelectric point of malachite was 7.3. After the addition of $Na_2S \cdot 9H_2O$, the zeta potential of malachite decreased, and changed slightly within the pH range of 1–3, thereafter, the zeta-potentials were significantly negatively charged. When $(NH_4)_2SO_4$ was added to strengthen the sulfidization, the zeta potential of malachite became more negative than that of malachite treated with $Na_2S \cdot 9H_2O$. This behavior may be attributed to the fact that the addition of $(NH_4)_2SO_4$ promotes the adsorption of more sulfide anions on the surface of malachite.

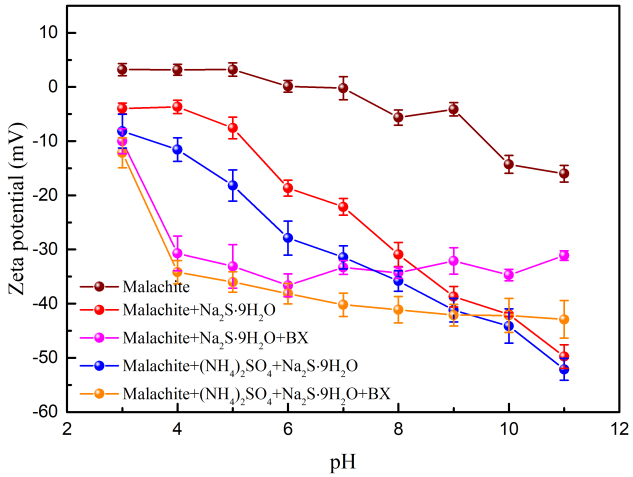

Fig. 8. Zeta potentials of malachite as function of pH in the absence and presence of $(NH_4)_2SO_4$, Na_2S and NaBX

After adding $Na_2S \cdot 9H_2O$ and BX to the solution, the zeta potential of the surface of malachite changed significantly within the pH range of 1–3. The results indicate a more negative potential than those from tests in which $Na_2S \cdot 9H_2O$ was added. The surface electricity of malachite becomes more negative, indicating that more anions are adsorbed on the mineral surface, which may be because of the adsorption of xanthate ions on the surface of malachite. When the pH was in the range of 3–7, the value of zeta potential tends to be stable, this may be due to the competitive adsorption between BX and sulfide anions.

3.2.3 SEM and AFM analysis

SEM and AFM were performed to explore the changes in the surface morphology of malachite before and after the sulfidizing reagents were added.

The SEM images shown in Fig. 9, it indicates that the surface of raw malachite is smooth and flat, and the fracture has sharp edges and corners. The EDS maps indicate that the malachite sample was very pure and that the weight and atom percentages (*wt*% and *at*%) of Cu on the surface of malachite were only 54.27% and 21.90%, respectively. Elemental S does not appear on the surface of malachite. After treatment with $Na_2S \cdot 9H_2O$, the surface of malachite has a layer of adhering material, particularly at the fault, which makes the edges and corners blunt. Through the EDS results, we found that there is elemental S on the surface of malachite, indicat that sulfides are attached to the surface of malachite. When $(NH_4)_2SO_4$ was added to enhance the sulfidation flotation of malachite, there are further attachment on the surface of malachite, and the edges and corners of the fracture layer are less apparent. The atom percentages of S increased from 0.12% to 0.16%, indicating that the addition of $(NH_4)_2SO_4$ promoted further adsorption of elemental S on the surface of the mineral.

AFM results show in Fig. 11. It can be seen in Fig. 11(a) that the surface of raw malachite is smooth, and no other substances are attached. The Fig. 11(b) show that after adding $Na_2S \cdot 9H_2O$ to the sulfidization reaction, the surface of malachite is covered with a layer of irregular material, which is speculated to be sulfide, but the formed sulfide material is loose and unevenly attached. After $(NH_4)_2SO_4$ and $Na_2S \cdot 9H_2O$ were added, it can be seen from Fig. 11(c) that the sulfuretted substances

that are obviously formed on the surface of malachite are more dense and denser than when directly sulfuretted in (b). And the distribution is more even. The result means that $(NH_4)_2SO_4$ can improve the stability of sulfide on the surface of minerals.

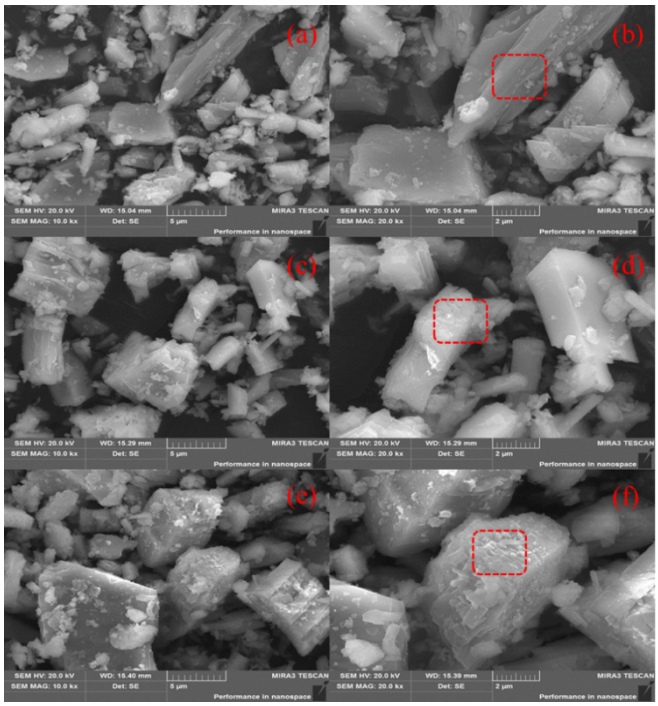

Fig. 9. SEM images of raw malachite(a)(b), malachite treated with $Na_2S \cdot 9H_2O$(c)(d), and malachite treated with $(NH_4)_2SO_4$ + $Na_2S \cdot 9H_2O$(e)(f)

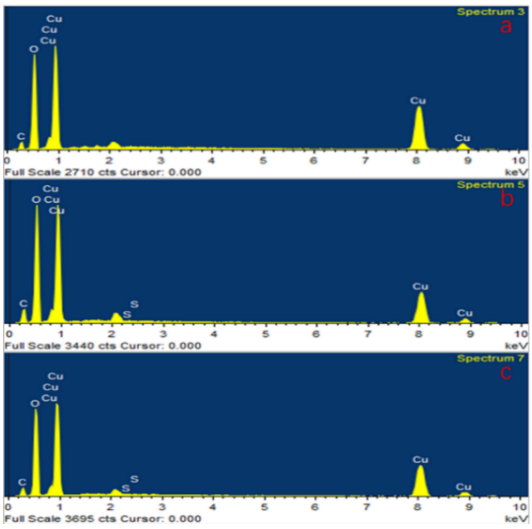

Fig. 10. EDS maps of (a) raw malachite, (b) malachite treated with $Na_2S \cdot 9H_2O$, and (c) malachite treated with $(NH_4)_2SO_4$ + $Na_2S \cdot 9H_2O$

Table 2. Results of EDS analyses (%)

Element	Malachite		Malachite + $Na_2S \cdot 9H_2O$		Malachite + $(NH_4)_2SO_4$ + $Na_2S \cdot 9H_2O$ 3	
	wt%	at%	wt%	at%	wt%	at%
CK	9.03	19.28	15.15	26.48	11.18	22.05
OK	36.70	58.82	46.29	60.73	40.43	59.84
SK	--	--	0.18	0.12	0.21	0.16
CuK	54.27	21.90	38.38	12.68	48.17	17.95

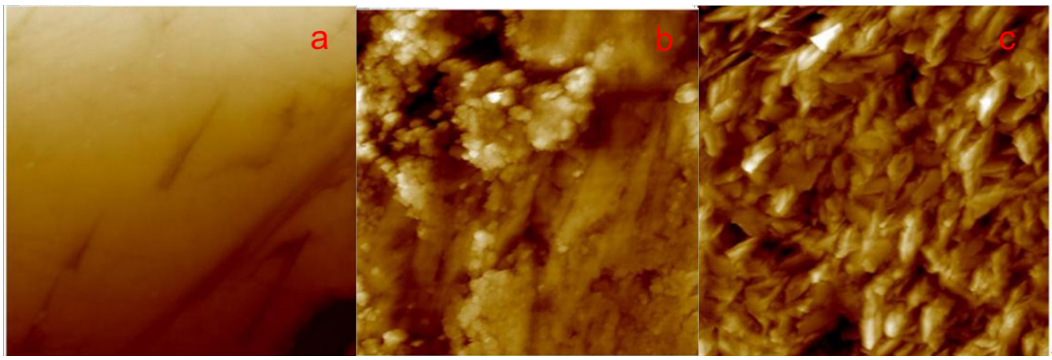

Fig. 11. AFM test of raw malachite(a) malachite treated with $Na_2S \cdot 9H_2O$(b), and malachite treated with $(NH_4)_2SO_4$ + $Na_2S \cdot 9H_2O$(c)

3.2.4. XPS analysis

The S 2p spectrum clearly demonstrates that S exists in multiple oxidation states, including the monosulfide (S^{2-}), polysulfide (Sn^{2-})/elemental S (S^0), sulfite (SO_3^{2-}) and sulfate (SO_4^{2-}) states (Gan et al., 2019a; Gan et al., 2019b).

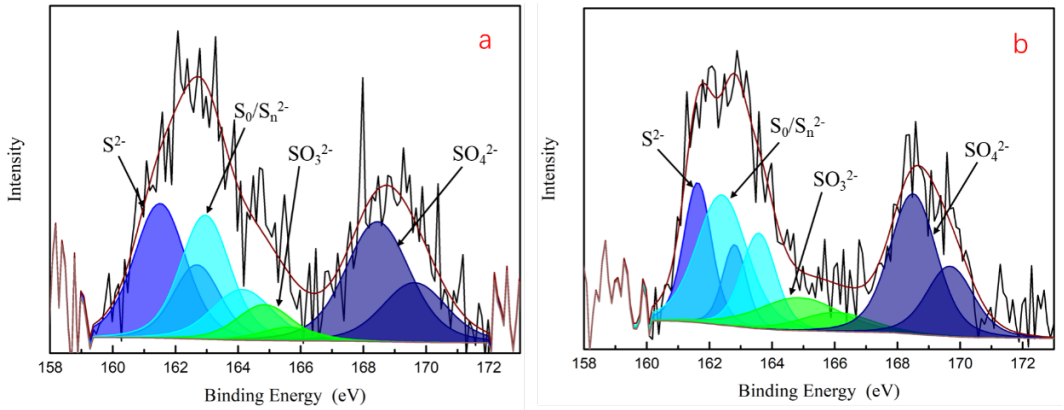

Fig. 12. S 2*p* spectra of malachite treated with (a) $Na_2S \cdot 9H_2O$ and (b) $(NH_4)_2SO_4$ + $Na_2S \cdot 9H_2O$

Table 3. S 2*p* XPS results for malachite

Species	Concentration (at%) (treated with $Na_2S \cdot 9H_2O$)	Concentration (at%) (treated with $(NH_4)_2SO_4$ + $Na_2S \cdot 9H_2O$)
S^{2-}	30.65	19.81
S_0/Sn^{2-}	26.99	33.21
SO_3^{2-}	8.66	13.63
SO_4^{2-}	33.70	33.35

Fig. 12 presents the S 2p spectrum of malachite after sulfidization and enhanced sulfidization. The XPS profile of sulfuretted malachite exhibits four groups of peaks in the S 2p electronic spectra located at 161.51, 162.95, 164.84, and 168.45 eV (Chen et al., 2014; Feng et al., 2017). Previous studies have reported that S 2p peaks with binding energy ranging from 161.2 to 162.3 eV represent divalent sulfide ions (S^{2-}) (Smart et al., 1999), whereas peaks with higher binding energy (162.4–164.3 eV) represent polysulfide ions (Sn^{2-}, $n \geq 2$) and peaks with binding energy ranging from 164.5 to 167.1 eV correspond to SO_3^{2-} ions. The peaks with binding energy of 167.8 and 169.9 eV correspond to the sulfate ion (SO_4^{2-}). After enhanced sulfidation, the XPS profiles of malachite also exhibit four groups of peaks in the S 2p electron spectrum. No new S peaks appeared, indicat that no new sulfide species were generated. Compared with Fig. 12(a) and 12(b), the intensities of the peaks had variations.

Table 3 presents the surface sulfur concentration of malachite after sulfidation and enhanced sulfidation. It can be seen that, compared with the surface of malachite treated with $Na_2S \cdot 9H_2O$, the addition of $(NH_4)_2SO_4$ to enhance sulfidation led to a decrease in the concentration of S^{2-} ions on the

surface of malachite from 30.65% to 19.81%. This implies that the addition of ammonium sulfate can promote the further oxidation of elemental sulfur.

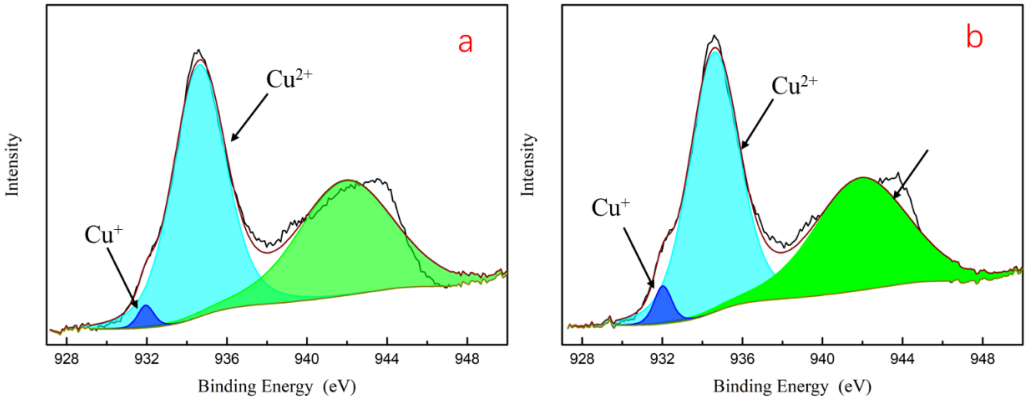

Fig. 13. Cu 2*p* spectra of malachite treated with (a) $Na_2S \cdot 9H_2O$ and (b) $(NH_4)_2SO_4$ + $Na_2S \cdot 9H_2O$

Fig. 13 displays the Cu 2p spectra of malachite after sulfidation and enhanced sulfidation. Both Cu (I) (cuprous) and Cu (II) (cupric) species were observed in Fig. 13 based on their distinct binding energy of 932.01 and 934.58 eV, respectively (A et al., 2014; Kartio et al., 1998; Li et al., 2015). Although no new peaks were apparent in the figure, a change in the intensity of the peak can be seen.

Table 4 list the concentration of copper on the surface of malachite after various treatments. It can be concluded that after adding $(NH_4)_2SO_4$ to strengthen the sulfidation of malachite, the concentration of Cu^+ ions on the surface of malachite were increased and that of Cu^{2+} ions were decreased. This implies that more Cu^{2+} ions are reduced to Cu^+ ions. This result is consistent with that obtained from the S 2p spectrum. The results of XPS indicate that a redox reaction occurs between sulfur and copper on the surface of malachite and that malachite sulfidation is a chemical reaction. The addition of $(NH_4)_2SO_4$ can enhance the redox reaction between malachite and $Na_2S \cdot 9H_2O$.

Table 4. Cu 2*p* XPS results for malachite

Species	Concentration (at%) (treated with $Na_2S \cdot 9H_2O$)	Concentration (at%) (treated with $(NH_4)_2SO_4$+ $Na_2S \cdot 9H_2O$)
Cu^+	2.68	4.92
Cu^{2+}	97.32	95.08

3.2.5. Computation results

We selected the (-201) surface of malachite as the main research object of this study. First, the structure of the malachite crystal cell model was optimized, and the optimized structure was cut out of the (-201) surface with three atomic layers. A 20 Å-thick vacuum layer was constructed. Fig. 14 presents the top and side views of the malachite (−201) surface.

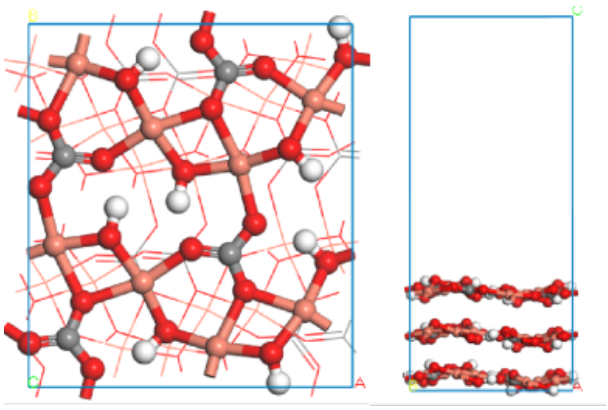

Fig. 14. Malachite (-201) surface

We placed ions on the optimized malachite (-201) surface to simulate and calculate the interaction process. The formula used to calculate the adsorption energy of atoms adsorbed on the surface of malachite is expressed as follows:

$$E_{ads} = E_{malachite+x} - E_{malachite} - E_x \quad (1)$$

where $E_{malachite}$ and $E_{malachite+x}$ represents the total energy before and after the atoms are adsorbed on the malachite (-201) surface, respectively, E_x represents the energy of each ion, and E_{ads} represents the adsorption energy. A negative E_{ads} value indicates that the reaction can proceed spontaneously. The more negative the value, the easier the reaction.

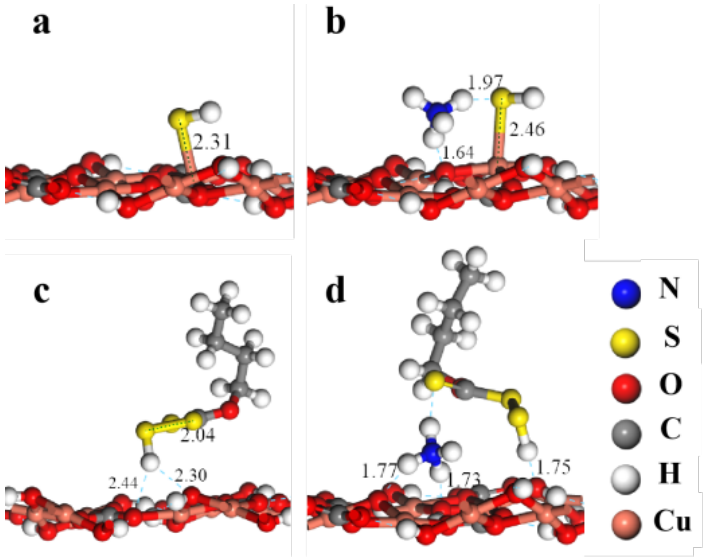

Fig. 15. Adsorption configurations of (a) HS^- ions, (b) HS^- and NH_4^+ ions, (c) HS^- and BX, and (d) HS, NH_4^+, and BX on malachite (−201) surface

Fig. 15(a) depicts the adsorption configuration of HS^- ions on the surface of malachite. We can see that the S atom of the HS^- ion interacts with the Cu atom and adsorbs on the surface of malachite to form a new bond. Fig. 15(b) presents the configuration of HS^- ions adsorbed on the surface of malachite after NH_4^+ added. The figure indicates that there is a strong hydrogen bond between NH_4^+ ions and the surface of malachite and HS^- ions. Fig. 15(c) presents the adsorption configuration of BX and HS- on the surface of malachite. It can be seen that BX uses the HS^- ions as a bridge to react with the surface of malachite. Fig. 15(d) depicts the adsorption configuration of NH_4^+, HS^-, and BX on the surface of malachite. By comparing the structure with that without NH_4^+ ions, it was found that after NH_4^+ added, the bond length between the HS^- ions and the surface of malachite was shortened significantly, indicating that the HS^- ions exert a stronger force on the surface of malachite.

Table 5 presents the adsorption energy of each type of ion on the surface of malachite. By comparison, after addition of NH_4^+ ions, the adsorption energy of HS^- ions on the surface of malachite become significantly negative, indicating that NH_4^+ ions are beneficial for the adsorption of HS^- ions on the surface of malachite. Moreover, considering the effect of the ammonium ion, the adsorption energy of BX dropped from -282.34 to -494.23 kJ/mol. This result indicates that HS^- and BX are adsorbed more stably on the surface of malachite after strengthening sulfidation.

Table 5. Adsorption energy of various agents

Model	Adsorption energy of various agents (kJ/mol)
HS^- ions	-91.26
HS^- ions (after strengthening sulfidation)	-139.41
Butyl xanthate (after sulfidation)	-282.34
Butyl xanthate (after strengthening sulfidation)	-494.23

4. Conclusions

(1) The addition of the sulfidizing agent and BX, is an effective method to improve the hydrophobicity of malachite, which is conducive to the flotation of malachite. Using $(NH_4)_2SO_4$ as accelerant, the recovery of malachite remarkably increases by 10%.

(2) Sulfidization mainly occurs at the surface fracture of malachite, and the addition of $(NH_4)_2SO_4$ can improve the efficiency of sulfidization and improve the stability of sulfide on the surface of malachite.

(3) The sulfurization reaction on the surface of malachite is a redox reaction. The addition of ammonium sulfate can promote the reaction and improve the curing efficiency of the surface of malachite.

(4) Computational results indicated that BX used HS^- ions as a bridge to react with the surface of malachite. After add $(NH_4)_2SO_4$, the adsorption energies of HS^- and BX on the surface of malachite became significantly negative. HS^- and BX were adsorbed more stably on the surface of malachite.

Acknowledgments

This research was supported by the National Natural Science Foundation of China (41773089); Foundation of the State Key Laboratory of Comprehensive Utilization of LowGrade Refractory Gold Ores (Zijin Mining Group Co.,Ltd, Shanghang 364200, China) (No. ZJKY2017(B)KFJJ004); Major Special Fund of Hunan Provincial Department of Science and Technology (2018GK1030) and the National Science Foundation of China (5207041966).

References

CAO, Z.F., ZHONG, H., LIU, G.Y., ZHAO, S.J., 2009. *Techniques of copper recovery from Mexican copper oxide ore.* Mining Science & Technology, 45-48.

CASTRO, S., SOTO, H., GOLDFARB, J., LASKOWSKI, J., 1974. *Sulphidizing reactions in the flotation of oxidized copper minerals, II. Role of the adsorption and oxidation of sodium sulphide in the flotation of chrysocolla and malachite*. International Journal of Mineral Processing 1, 151-161.

CHEN, X., PENG, Y., BRADSHAW, D., 2014. *The separation of chalcopyrite and chalcocite from pyrite in cleaner flotation after regrinding*. Minerals Engineering 58, 64-72.

CLARK, S.J., SEGALL, M.D., PICKARD, C.J., HASNIP, P.J., PROBERT, M.J., REFSON, K., PAYNE, M.C., 2005. *First principles methods using CASTEP*. Zeitschrift Fur Kristallographie 220, 567-570.

CORIN, K.C., KALICHINI, M., O'CONNOR, C.T., SIMUKANGA, S., 2017. *The recovery of oxide copper minerals from a complex copper ore by sulphidisation*. Minerals Engineering 102, 15-17.

EJTEMAEI, M., GHARABAGHI, M., IRANNAJAD, M., 2014. *A review of zinc oxide mineral beneficiation using flotation method.* Adv Colloid Interface, 206, 68-78.

FENG, Q.C., WEN, S.M., 2017. *Formation of zinc sulfide species on smithsonite surfaces and its response to flotation performance.* Journal of Alloys & Compounds 709, 602-608.

FENG, Q.C., WEN, S.M., ZHAO, W.J., LV, C., BAI, X., 2015. *Leaching of Copper from Malachite with Methane-sulfonic Acid*. Solvent Extraction Research and Development-Japan 22, 159-168.

FROST, R.L., XI, Y., WOOD, B.J., 2012. *Thermogravimetric analysis, PXRD, EDX and XPS study of chrysocolla (Cu,Al)2H2Si2O5(OH)4·nH2O : structural implications.* Thermochimica Acta 545, 157-162.

FUERSTENAU, D.W., HERRERA-URBINA, R., MCGLASHAN, D.W., 2000. *Studies on the applicability of chelating agents as universal collectors for copper minerals*. International Journal of Mineral Processing 58, 15-33.

GAN, M., GU, C., DING, J., ZHU, J., LIU, X., QIU, G., 2019a. *Hexavalent chromium remediation based on the synergistic effect between chemoautotrophic bacteria and sulfide minerals*. Ecotoxicol Environ Saf 173, 118-130.

GAN, M., HE, P., GU, C., ZHENG, Z., ZHU, J., ZHOU, S., LIU, X., QIU, G., 2019b. *Graphene and visible light enhance pyrite-based Cr(VI) reduction in the presence of Acidithiobacillus ferrooxidans*. International Biodeterioration & Biodegradation 137, 78-87.

HOPE, G.A., BUCKLEY, A.N., PARKER, G.K., NUMPRASANTHAI, A., WOODS, R., MCLEAN, J., 2012. *The interaction of n-octanohydroxamate with chrysocolla and oxide copper surfaces*. Minerals Engineering 36-38, 2-11.

HU, Y., QIU, G., YUAN, C., WANG, D., 1996. Solution chemistry studies on flotation of malachite and smithsonite. Nonferrous Metals.

Kartio, I.J., Basilio, C.I., Yoon, R.H., 1998. *An XPS study of sphalerite activation by copper.* Langmuir 14, 5274-5278.

LEE, J.S., NAGARAJ, D.R., COE, J.E., 1998. *Practical aspects of oxide copper recovery with alkyl hydroxamates.* Minerals Engineering 11, 929-939.

LI, F., HONG, Z., XU, H., HUI, J., LIU, G., 2015. *Flotation behavior and adsorption mechanism of a-hydroxyoctyl phosphinic acid to malachite.* Minerals Engineering 71, 188-193.

LI, Z., RAO, F., SONG, S., 2017. *Comparison of Adsorption of Phenol O-O and N-O Chelating Collectors at the Malachite/Water Interface in Flotation,* Minerals, 7(2), 20.

LIU, C., FENG, Q., ZHANG, G., 2018. *Effest of ammonium sulfate on the sulfidation flotation of malachite.* Archives of mining sciences 63, 139-148.

LIU, M., ZHANG, C., HU, B., SUN, Z., XU, Q., WEN, J., XIAO, J., DONG, Y., GAN, M., SUN, W., 2020. *Enhancing flotation separation of chalcopyrite and galena by the surface synergism between sodium sulfite and sodium lignosulfonate.* Applied Surface Science, 507, 145042.

LIU, R., LIU, D., LI, J., LI, J., NING, S., 2020. *Sulfidization mechanism in malachite flotation: A heterogeneous solid-liquid reaction that yields CuxSy phases grown on malachite*. Minerals Engineering 154, 106420.

LIU, R., LIU, Z., LI, J., AO, S., LI, J., 2020. *Reexamining the Role of Ammonium Ions in the Sulfidization, Xanthate-Flotation of Malachite*. Minerals 10, 537.

NAGARAJ, D.R., FARINATO, R.S., 2016. *Evolution of flotation chemistry and chemicals: A century of innovations and the lingering challenges*. Minerals Engineering, 2-14.

NAKLICKI, M.L., RAO, S.R., GOR, M., FINCH, J.A., 2002. *Flotation and surface analysis of the nickel (II) oxide/amyl xanthate system*. International Journal of Mineral Processing, 65, 73-82.

SHEN, P., LIU, D., ZHANG, X., JIA, X., SONG, K., LIU, D., 2019. *Effect of (NH4)(2)SO4 on eliminating the depression of excess sulfide ions in the sulfidization flotation of malachite.* Minerals Engineering 137, 43-52.

SHENGO, L.M., GAYDARDZHIEV, S., KALENGA, N.M., 2014. *Assessment of water quality effects on flotation of copper-cobalt oxide ore*. Minerals Engineering 65, 145-148.

SMART, R.S., SKINNER, W.M., GERSON, A.R., 1999. *XPS of sulphide mineral surfaces: Metal-deficient, polysulphides, defects and elemental sulphur*. Surface and Interface Analysis 28, 101-105.

TANDA, B.C., EKSTEEN, J.J., ORABY, E.A., 2017. *An investigation into the leaching behaviour of copper oxide minerals in aqueous alkaline glycine solutions*. Hydrometallurgy 167, 153-162.

TRAN, M., ROY, S., KMIEC, S., WHALE, A., MARTIN, S., SUNDARARAJAN, S., PADALKAR, S., 2020. *Formation of Size and Density Controlled Nanostructures by Galvanic Displacement.* Nanomaterials 10, 15.

WU, D., MA, W., MAO, Y., DENG, J., WEN, S., 2017a. E*nhanced sulfidation xanthate flotation of malachite using ammonium ions as activator*. Scientific Reports 7, 2086.

WU, D., MAO, Y., DENG, J., WEN, S., 2017b. *Activation mechanism of ammonium ions on sulfidation of malachite (-201) surface by DFT study*. Applied Surface Science 410, 126-133.

XU, J., 1989. New collector for the flotation of wolframite. Nonferrous Metals.

YANG, X., LIU, S., LIU, G., ZHONG, H., 2017. *A DFT study on the structure-reactivity relationship of aliphatic oxime derivatives as copper chelating agents and malachite flotation collectors.* Journal of Industrial and Engineering Chemistry 46, 404-415.

ZHANG, L., 2008. *Basic Research and Application of Flotation in Tonglushan Copper Mine.* Central South University.

ZHANG, W.B., POLING, G.W., 1989. *Ammonium sulphate as activator in sulphidized xanthate flotation of malachite*. CIM Bulletin 82, 35–39.